In-Reactor Polypropylene Functionalization-The Influence of Catalyst Structures and Reaction Conditions on the Catalytic Performance

Bouyahyi, Miloud; Jasinska-Walc, Lidia; Duchateau, Rob; Akhtar, Muhammad Naseem; Jaseer, E. A.; Theravalappil, Rajesh; Garcia, Nestor

Published in:
Macromolecules

DOI:
10.1021/acs.macromol.1c02220

Publication date:
2022

Macromolecules

pubs.acs.org/Macromolecules Article

In-Reactor Polypropylene Functionalization—The Influence of Catalyst Structures and Reaction Conditions on the Catalytic Performance

Miloud Bouyahyi,* Lidia Jasinska-Walc, Rob Duchateau,* Muhammad Naseem Akhtar,* E. A. Jaseer, Rajesh Theravalappil, and Nestor Garcia

Cite This: *Macromolecules* 2022, 55, 776−787 Read Online

ACCESS | Metrics & More | Article Recommendations | Supporting Information

ABSTRACT: To unravel the relationship between silylene-bridged metallocene catalyst structures and polymerization conditions and their effect on the performance in in-reactor functionalization of polypropylene, the behaviors of *rac*-Me_2Si(2-Me-4-Ph-Ind)$_2ZrCl_2$/MMAO, *rac*-$Me_2Si(Ind)_2ZrCl_2$, *rac*-Me_2Si(2-Me-4-Ph-Ind)$_2HfCl_2$, and *rac*-$Me_2Si(Ind)_2HfCl_2$ in propylene/aluminum alkyl-passivated 10-undecen-1-ol copolymerization were compared. Kinetic analysis revealed higher catalytic activities for zirconocenes compared to analogous hafnocenes. Both the zirconocene and hafnocene with substituted indenyl ligands afforded a higher molecular weight capability, improved stereo-selectivity, and enhanced ability to incorporate functionalized comonomers compared to their non-substituted congeners. An in-depth study of polypropylene functionalization using the best performing catalyst system, *rac*-Me_2Si(2-Me-4-Ph-Ind)$_2ZrCl_2$/MMAO, at temperatures ranging from 40 to 100 °C, revealed a linear inversely proportional correlation of polymerization temperature with functionalized comonomer reactivity ($\uparrow T_p \rightarrow \downarrow r_1$), copolymer molecular weight ($\uparrow T_p \rightarrow \downarrow M_n$), and melting temperature ($\uparrow T_p \rightarrow \downarrow T_m$). While performing well under standard laboratory polymerization conditions, *rac*-Me_2Si(2-Me-4-Ph-Ind)$_2ZrCl_2$/MMAO showed limited molecular weight and stereo-selectivity capabilities under high-temperature (130−150 °C) solution process conditions. Although immobilization of *rac*-Me_2Si(2-Me-4-Ph-Ind)$_2ZrCl_2$ onto silica, allowing it to be used under industrially relevant slurry and gas-phase conditions, led to an active catalyst, it failed to incorporate any functionalized comonomer.

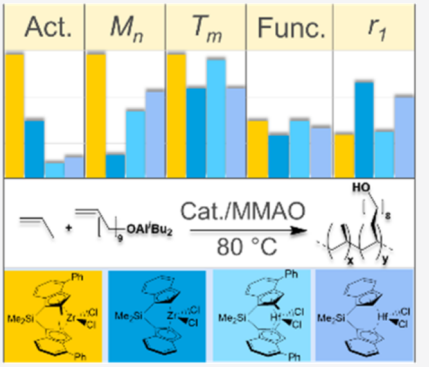

INTRODUCTION

Polyolefins form the cheapest and most abundantly used class of all polymers. With only a handful of monomers, materials with a wide variety of properties have been obtained ranging from elastomers to thermoplastics. Even the structurally simple linear polyethylene finds use in a wide range of applications from grocery bags to bullet proof vests or medical implants. Tuning the polymer's topology broadens its potential even more, resulting in, for example, high-temperature-resistant thermoplastic elastomers and shape memory materials.[1−3] However, one feature that all these fantastic materials lack is functionality: polyolefins are aliphatic hydrocarbons that are chemically inert and have a very low surface energy. Combining the polyolefins' excellent mechanical properties with the ability to adhere to other materials is of great interest, and significant effort has been directed toward the development of various approaches to produce functionalized polyolefins.[4−6]

Besides surface modification of polyolefin devices by, for example, corona- or flame treatment,[7] polyolefins can be functionalized either by post-reactor or in-reactor functionalization processes.[8] The post-reactor process typically consists of reactive extrusion using a polyolefin, a functional group to be grafted, and typically a radical initiator.[9] In-reactor functionalization is performed on a commercial scale for producing functionalized polyethylenes using a high-pressure radical process. Although catalytic in-reactor functionalization of polyolefins is frequently being reported in scientific publications and patents,[4−6,10,11] no commercial scale process exists to date.

In-reactor functionalization of polyolefins has been reported in the literature using various catalytic approaches. For examples, multi-step processes consisting of (i) coordinative chain-transfer polymerization followed by selective oxidation of the metal carbon bond to produce chain-end functionalized polyolefins,[12,13] (ii) copolymerization of olefins with comonomers containing latent reactive groups such as substituted styrenes and their derivatives followed by a post-polymer-

Received: October 26, 2021
Revised: December 20, 2021
Published: January 26, 2022

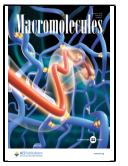

https://doi.org/10.1021/acs.macromol.1c02220
Macromolecules 2022, 55, 776−787

Chart 1. Catalyst Precursors Used for the Copolymerization of Propylene/TiBA-Passivated 10-Undecen-1-ol

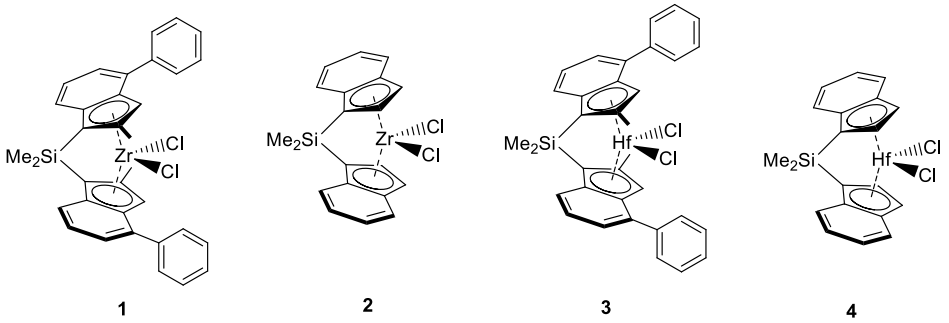

Table 1. Results of Propylene Copolymerization with $C_{11}{}^{=}O\text{-}Al^{i}Bu_2$ Catalyzed by 1−4/MMAO Catalyst Systems at 80 °C[a]

run #	cat.	cat. (μmol)	$C_{11}{}^{=}O\text{-}Al^{i}Bu_2$[b] (mM)	yield (g)	activity (kg mmol cat.$^{-1}$ h^{-1})	M_n[c] (kg mol^{-1})	$Đ$[c]	T_m[d] (°C)	$C_{11}OH$[e] (mol %)
1	**1**	0.06	0	26.4	1320	80.5	3.0	154.7	0
2		0.06	10	15.6	782	127.4	2.3	152.4	0.2
3		0.06	20	5.4	269	162.6	2.4	150.6	0.4
4		0.06	40	5.0	252	127.5	2.8	141.8	0.8
5	**2**	0.32	0	21.7	203	12.1	2.3	130.0	0
6		0.32	10	16.0	150	14.3	2.4	129.4	0.1
7		0.32	20	13.3	125	14.8	2.3	129.0	0.2
8		0.32	40	11.5	108	15.8	2.3	126.1	0.5
9	**3**	1.86	0	9.6	16	40.6	3.3	152.8	0
10		1.86	10	8.2	13	40.7	3.1	148.6	0.2
11		1.86	20	6.9	11	43.8	3.2	146.3	0.4
12		1.86	40	7.5	12	45.8	3.1	140.8	0.8
13	**4**	1.86	0	14.3	23	69.7	3.2	129.7	0
14		1.86	10	12.0	19	44.9	4.9	129.2	0.1
15		1.86	20	11.6	19	82.9	2.6	129.5	0.3
16		1.86	40	7.4	12	54.5	3.5	125.9	0.6

[a]Conditions: reactions performed in a 600 mL Büchi reactor, 200 mL toluene, propylene pressure = 5 bar, [MMAO]/[cat. **1**] ∼ 8300, [MMAO]/[cat. **2**] ∼ 8092, [MMAO]/[cat. **3**] ∼ 4284, [MMAO]/[cat. **4**] ∼ 4284, TiBA (10 wt % solution in toluene) = 2.1 mmol, reaction time = 20 min. [b]10-Undecen-1-ol ($C_{11}{}^{=}OH$) premixed with TiBA (10 wt % solution in toluene; [TiBA]/[$C_{11}{}^{=}OH$] = 1.1). [c]Determined by HT-SEC in TCB at 160 °C. [d]Determined by DSC. [e]Determined by ^{1}H NMR.

ization functionalization step,[14] (iii) random incorporation of electrophile-functionalized comonomers such as borane[15] and aluminum[16] followed by oxidation, and (iv) direct copolymerization of propylene with nucleophile-functionalized comonomers typically passivated with silyl- or aluminum alkyl groups.[17,18] The latter is the most common route and has been proven efficient to produce functionalized polyolefins at a lab scale and provides access to a wider range of products with different types and amounts of functionality. This approach has been applied to produce copolymers of ethylene or α-olefins, with olefin comonomers bearing polar functionalities such as hydroxyls,[19−21] phenols,[22,23] carboxylic acids,[24−26] (thio)-esters,[27] epoxides,[28] and (thio)ethers[29] typically using single-site metallocene catalysts. Recently, unprotected amine- and anisyl-functionalized monomers have been directly copolymerized with ethylene and propylene using group 3−4 single-site metal-based catalysts to access amine-functionalized polyolefins.[30−33] Nevertheless, the presence of even small amounts of functionalized comonomers, including the passivated ones, typically has a negative effect on the catalytic activity of the highly electrophilic catalysts. The majority of the studies on functionalized polyolefins are focused on the catalytic performance in the presence of these (passivated) functionalized comonomers (catalytic activity and incorporation ability of functionalized comonomers).[34]

Since its publication by Spaleck et al. in 1994,[35] the unprecedented activity and isospecificity of *rac*-Me_2Si(2-Me-4-Ph-Ind)$_2ZrCl_2$ (**1**) in propylene polymerization have inspired many researchers to investigate the structure−property relationship of metallocenes and **1** has become a benchmark catalyst for many olefin (co)polymerization studies.[36−38] The "Spaleck catalyst" (**1**) has also been used to produce randomly functionalized polypropylenes.[39−41] Most of these publications described the use of **1** as a catalyst to produce functionalized polypropylenes, but little is known about its actual catalytic behavior when used as a catalyst to produce functionalized polyolefins, especially under industrially relevant conditions.

To be able to evaluate the true commercial potential of this catalyst in an in-reactor functionalization process, a thorough study under industrially relevant conditions is required. Specifically, this implies polymerization temperatures in the range of 60−90 °C for gas-phase or slurry processes and ≥130 °C for a solution process and polymerization times of >10 min to an hour, instead of only seconds at room temperature as performed by Cai and co-workers.[41]

No data exist on the catalytic performance of other metallocenes in the copolymerization of propylene and polar comonomers (i.e., alkenols) under industrially relevant conditions. Therefore, prior to exploring the potential of **1** for producing functionalized polyolefins under the gas-phase or solution process conditions, the performance of **1** was

https://doi.org/10.1021/acs.macromol.1c02220
Macromolecules 2022, 55, 776−787

compared with that of other silylene-bridged zirconium- and hafnium-based catalysts: *rac*-$Me_2Si(Ind)_2ZrCl_2$ (**2**), *rac*-Me_2Si-$(2\text{-Me-4-Ph-Ind})_2HfCl_2$ (**3**), and *rac*-$Me_2Si(Ind)_2HfCl_2$ (**4**) (Chart 1). The comparison was directed to the effect of the catalyst structure and polymerization conditions on the catalytic activity, incorporation ability of functionalized comonomers, molecular weight capability, and isospecificity.

MATERIALS AND METHODS

General Considerations. All experiments were performed under an inert dry nitrogen atmosphere using either standard Schlenk or glovebox techniques. All chemicals used were purchased from Sigma-Aldrich, for example, MMAO-12 (7 wt % solution in toluene), 10-undecene-1-ol, triisobutylaluminum (TiBA, neat), toluene—HPLC grade, and trityl tetrakis(pentafluorophenyl)borate. Propylene was purchased from Abdulla Hashim Gas Co. Saudi Arabia. *rac*-$Me_2Si(2\text{-Me-4-Ph-Ind})_2ZrCl_2$ (**1**), *rac*-$Me_2Si(Ind)_2ZrCl_2$ (**2**), *rac*-$Me_2Si(2\text{-Me-4-Ph-Ind})_2HfCl_2$ (**3**), and *rac*-$Me_2Si(Ind)_2HfCl_2$ (**4**) pre-catalysts were purchased from MCAT GmbH, Germany.

Random Copolymerization of Propylene and TiBA-Passivated 10-Undecen-1-ol Using 1−4 as Catalyst Precursors. The copolymerization reactions of propylene with TiBA-passivated 10-undecen-1-ol using catalyst precursors **1**−**4** and MMAO-12 "MMAO" as a co-catalyst were performed using a premixed solution of TiBA and $C_{11}{=}OH$ (molar ratio of $C_{11}{=}OH$/TiBA 1:1.1), yielding the protonolysis product, $C_{11}H_{21}OAl^iBu_2$ ($C_{11}{=}O\text{-}Al^iBu_2$). The copolymerization experiments were carried out in a 0.6 L stainless steel Büchi reactor system (assembled by Hi-Tech, India) equipped with a propeller-like stirrer. The reactor was evacuated and heated using an external oil bath. The reactor vessel was kept under vacuum at a temperature of 110 °C for 10 min to remove any condensed moisture. The reactor vessel was then purged with argon and vacuum several times. After this step, the reactor vessel was cooled to the required polymerization temperature. For example, as shown in entry 2, Table 1, the total volume of the polymerization medium was kept to approx. 200 mL, and the reactor was charged with the required amounts of toluene (200 mL)/MMAO-12 (7 wt % solution in toluene, 0.5 mL), TiBA solution (10 wt % solution in toluene, 2.1 mmol), and the solution of $C_{11}{=}O\text{-}Al^iBu_2$ (1 M solution in toluene, 1 mL, 5 mM). The mixture was then pre-saturated with propylene at a pressure of 5 bar and the required polymerization temperature (80 °C). Finally, the catalyst precursor solution in toluene (0.06 μmol) was injected into the reactor vessel applying an overpressure of argon of 0.5 bar. The polymerization started immediately upon the addition of the catalyst precursor. The stirring speed was kept at 500 rpm, and the polymerization was performed for 20 min. The polymerization temperature was maintained constant during the reaction by circulating hot oil in the reactor jacket and cooling liquid through a cooling spiral inside the reactor vessel. SCADA software was used to control the reaction temperature and pressure of the polymerization reactor precisely. The propylene consumption was followed using a mass flow controller to keep the pressure constant. At the end of the set time, the polymerization was stopped by depressurizing the reactor. The resulting mixture containing the polymer was then quenched with acidified methanol (200 mL, 5 mol % HCl), and subsequently, an acetone solution (5 mL) containing butylated hydroxytoluene (2,6-tBu$_2$-4-Me-C_6H_2OH, BHT) (30 g of BHT in 1 L acetone) was added, and the product mixture was stirred for 3 h. The polymer was then filtered, washed four times with demineralized water, filtered, and dried overnight in a vacuum oven at 60 °C to yield 15.2 g of poly(propylene-*co*-undecenol). The functionality content was determined by ^{1}H NMR, and a typical ^{1}H NMR of poly(propylene-*co*-undecenol) prepared using **1**/MMAO is shown in Figure S4. The relative integrated intensity ratio of the CH_2OH resonances and of methine proton $-CH_2CH(CH_3)-$ resonances of propylene repeating units (1.6 ppm) was used to determine the incorporation of $C_{11}{=}OH$.

Slurry Phase Copolymerization of Propylene and TiBA-Passivated 10-Undecen-1-ol Using Silica Supported 1. A similar polymerization procedure was applied in propylene copolymerization with TiBA-pacified 10-undecen-1-ol catalyzed by the silica-supported *rac*-$Me_2Si(2\text{-Me-4-Ph-Ind})_2ZrCl_2$ catalyst (**1**).

Gas-Phase Conditions. 50 mg of silica-supported **1** was pre-mixed with paraffin oil (16.7 wt %) and TiBA (1.0 M solution in hexane, 1 mL) at a propylene pressure = 20 bar and at a reaction time = 60 min. 10-Undecen-1-ol ($C_{11}{=}OH$) was pre-mixed with TiBA (1 M solution in toluene; [TiBA]/[$C_{11}{=}OH$] = 1.0).

Slurry-Phase Conditions. 10 mg of silica-supported **1**, heptane (275 mL), and TiBA (1.0 M solution in hexane, 1 mL) were pre-mixed at a propylene pressure = 5 bar and at a reaction time = 40 min. 10-Undecen-1-ol ($C_{11}{=}OH$) was pre-mixed with TiBA (1 M solution in toluene; [TiBA]/[$C_{11}{=}OH$] = 1.0).

The supported catalyst **1**/SiO_2 was prepared following the conditions described in ref 42.

Analytical Techniques. *High-Temperature Size Exclusion Chromatography.* The molar mass and molar mass distribution of the polymers were determined using an SEC instrument (PL-GPC 220, Agilent Technologies). The SEC instrument was equipped with two PLgel Olexis 300 × 7.5 mm columns, and the analysis of polymer samples was performed at 160 °C. 1,2,4-Trichlorobenzene was used as the solvent. BHT (0.0125 wt %) was added to 1,2,4-trichlorobenzene to prevent the degradation of the polymer samples. A sample solution of approximately 2 mg mL^{-1} was prepared at 170 °C using a PL-SP260 sample preparation unit equipped with a heater and shaker. A sample volume of 100 μL was injected into the SEC columns. The columns were calibrated using narrow mass distribution polystyrene standards using the universal calibration method. The chromatographic data were analyzed using the Agilent GPC/SEC software. The polystyrene-based calibration curve was converted into the universal one using the Mark−Houwink constants of polystyrene (K = 0.000121 dL g^{-1} and α = 0.707) and polypropylene (K = 0.000135 dL g^{-1} and α = 0.750).

Nuclear Magnetic Resonance Spectroscopy. The samples were dissolved at 130 °C in deuterated tetrachloroethane (TCE-d_2) containing BHT as the stabilizer. The spectra were recorded in 5 mm tubes on a Bruker AVANCE 500 spectrometer equipped with a cryogenically cooled probe head operating at 125 °C. Chemical shifts are reported in ppm versus the residual solvent protons.

Differential Scanning Calorimetry. Differential scanning calorimetry (DSC) experiments were conducted using a TA DSC Q2000 instrument. The temperature and heat flow of the apparatus were calibrated with an indium standard. For the DSC analysis, the specimens were heated in a nitrogen atmosphere (flow rate 50 mL min^{-1}) at 10 °C min^{-1}. A sample of about 5−10 mg was used for the experiment, and the T_m values were determined from the second heating cycle.

RESULTS AND DISCUSSION

Copolymerization of Propylene with $C_{11}{=}O\text{-}Al^iBu_2$ Using Catalysts 1−4/MMAO. The first series of experiments focused on the optimization of the catalyst loading to operate under isothermal conditions in propylene polymerization. The concentration of **1** had to be lowered to 0.3 μM to achieve well-controlled isothermal propylene polymerization experiments, giving reproducible yields and polymer molecular weights. Due to the inherent deactivation of early transition-metal-based catalysts by polar comonomers, 10-undecen-1-ol ($C_{11}{=}OH$) had to be passivated with TiBA, and the catalyst loading had to be adjusted during propylene/$C_{11}{=}O\text{-}Al^iBu_2$ copolymerization to produce acceptable amounts of functionalized polypropylenes (vide infra). The effect of the co-catalyst type and amount was also investigated, and the optimum balance between the catalyst activity and product properties (MW, T_m) was achieved using the MMAO co-catalyst (see the Supporting Information for details).

https://doi.org/10.1021/acs.macromol.1c02220
Macromolecules 2022, 55, 776−787

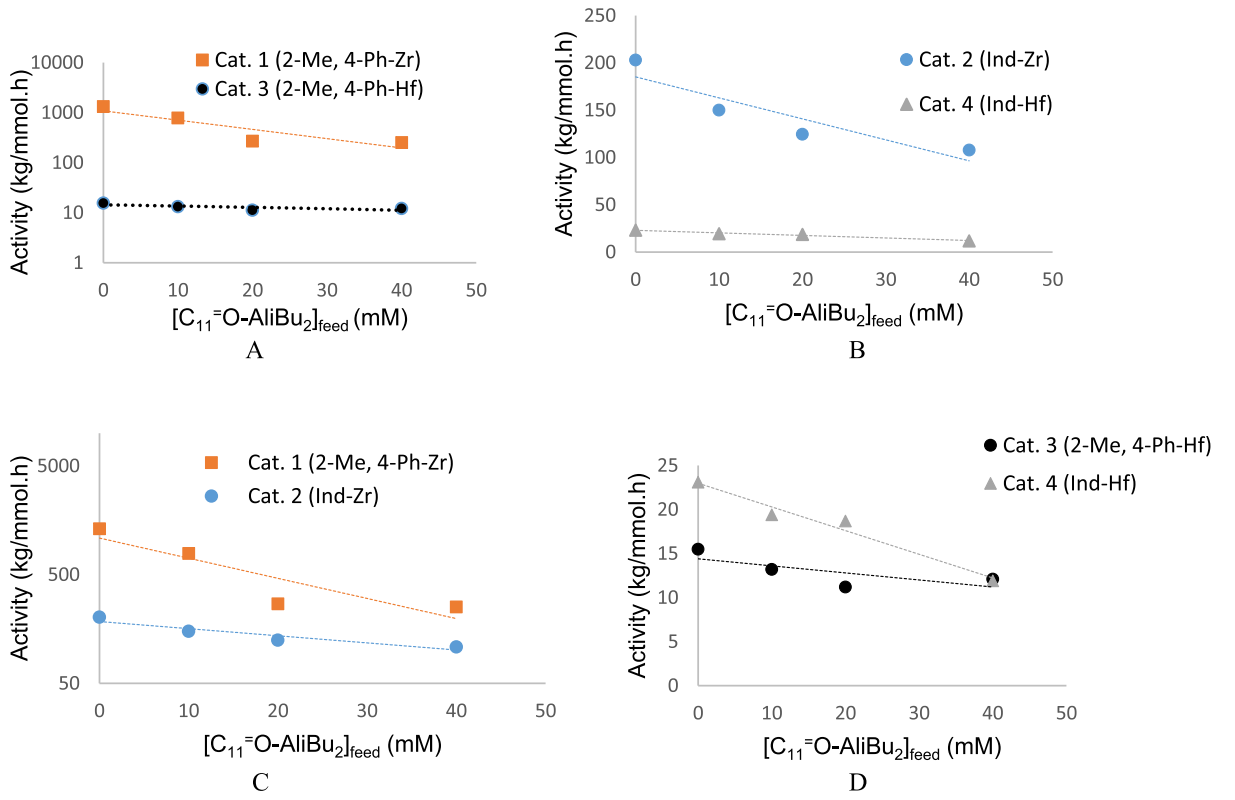

Figure 1. Comparison of the catalytic activity against the feed concentration of $C_{11}{=}O\text{-}Al^iBu_2$ in propylene/$C_{11}{=}O\text{-}Al^iBu_2$ copolymerization at 80 °C catalyzed by **1**−**4**/MMAO: (A) metal center effect of **1** vs **3**; (B) metal center effect of **2** vs **4**; (C) ligand effect of **1** vs **2**; (D) ligand effect of **3** vs **4**.

Attempting to understand the effect of the catalyst structure on its catalytic performance in propylene/$C_{11}{=}O\text{-}Al^iBu_2$ copolymerization (catalytic activity and copolymer properties), three additional catalyst precursors have been selected based on their structural similarities with **1**: pre-catalyst **2**, which is the unsubstituted bis(indenyl) congener of **1**; complex **3**, which has the same ligand structure as **1** but with hafnium as the metal; complex **4**, which is the unsubstituted bis(indenyl) analogue of **3**. The comparative copolymerizations of propylene and $C_{11}{=}O\text{-}Al^iBu_2$ have been conducted at a fixed polymerization temperature (80 °C) and propylene pressure (5 bar), and the results are summarized in Table 1.

At a lower $C_{11}{=}O\text{-}Al^iBu_2$ feed concentration (up to 10 mM), the catalytic activities of the zirconium-based catalysts **1** and **2** are at least an order of magnitude higher than that of the hafnium-based analogues **3** and **4**, respectively (Figure 1A,B). This observation is in line with literature data, commonly reporting higher catalytic activities of zirconocenes than analogous hafnocenes in olefin polymerization.[43,44] Increasing the $[C_{11}{=}O\text{-}Al^iBu_2]$ feed concentration (>10 mM) resulted in a clear negative effect on catalytic activities for all catalysts **1**−**4**, irrespective of the catalyst metal center or ligand structure.

This relative drop in catalytic activity seems, however, to be more pronounced for the zirconium-based catalysts **1** and **2**. As a result of its initial higher catalytic activity, the deactivation of **1** seems the strongest, but even with the highest feed concentrations of $C_{11}{=}O\text{-}Al^iBu_2$ (40 mM), the catalytic activity of **1** is still significantly higher than for **2**−**4** during propylene homopolymerization. Comparing the catalytic activity of the reference polymerization experiments for **1**−**4** with the average catalytic activity for the three last entries for each catalyst where $[C_{11}{=}O\text{-}Al^iBu_2] \geq 20$ mM shows a comparable drop in activity for **2** and **4** (40−50%), and the lowest deactivation was observed using **3** (∼20%). The comparison of the ligand effect for **1**−**4** did not show a distinct trend with overall higher catalytic activities observed using the zirconium-based catalyst bearing the substituted indenyl ligand **1** (Figure 1C), and the opposite trend was observed with hafnium-based catalysts **3** and **4**, with a higher catalytic activity displayed by **4** (Figure 1D).

The ability of **1**−**4** to incorporate $C_{11}{=}O\text{-}Al^iBu_2$ was analyzed by ^{1}H NMR, and a typical ^{1}H NMR of poly(propylene-*co*-undecenol) prepared using **1**/MMAO is shown in Figure S4. The methylene protons of the CH_2OH showed a clear triplet at 3.6 ppm. Plotting the $C_{11}{=}OH$ content versus the $[C_{11}{=}O\text{-}Al^iBu_2]_{feed}$ (Figure 2) clearly demonstrates the effect of the catalyst structure on its ability to incorporate $C_{11}{=}O\text{-}Al^iBu_2$. Higher functionality levels were obtained for the zirconocene and hafnocene bearing the substituted indenyl ligand (**1** vs **2**; **3** vs **4**). This is in line with the observed higher α-olefin incorporation during ethylene/α-olefin copolymerization using substituted bis(indenyl) catalysts versus their unsubstituted analogues.[43] During ethylene/α-olefin copolymerization, hafnocenes typically give a higher α-olefin incorporation than structurally similar zirconocenes.[45] In our study, the effect of the metal is most clearly visible for the unsubstituted metallocenes where hafnocene **4** indeed incorporates $C_{11}{=}O\text{-}Al^iBu_2$ better than the zirconocene **2**. The difference for **1** and **3** is less clear.

The plot of the melting temperature versus the $C_{11}{=}O\text{-}Al^iBu_2$ feed concentration confirms the efficient incorporation of $C_{11}{=}OH$ using catalysts **1**−**4**, with functionality levels

https://doi.org/10.1021/acs.macromol.1c02220
Macromolecules 2022, 55, 776−787

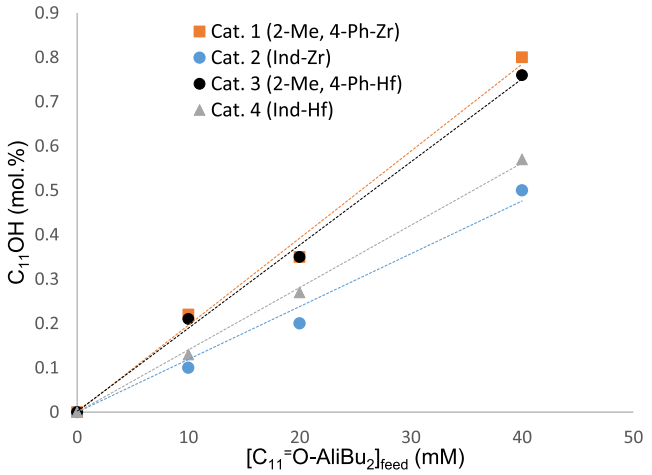

Figure 2. Plot of $C_{11}{}^{=}OH$ content (mol %) of poly(propylene-*co*-undecenol) copolymers prepared using catalysts **1**–**4** against the feed concentration of $C_{11}{}^{=}O\text{-}Al^{i}Bu_2$ (mM) at 80 °C.

increasing linearly with the increase of the $C_{11}{}^{=}O\text{-}Al^{i}Bu_2$ feed concentration at a constant propylene concentration, in agreement with the pseudo-first-order kinetics of a semi-batch experiment. The effect of the catalyst structure is clearly demonstrated in Figure 3, where the plots of the melting temperature against the $[C_{11}{}^{=}O\text{-}Al^{i}Bu_2]_{feed}$ (Figure 3A) and comonomer content (Figure 3B) obtained using substituted catalysts **1** and **3** reveal a clear distinction compared to those obtained using the unsubstituted catalysts **2** and **4**. The linear inverse correlation between the melting temperatures and the $[C_{11}{}^{=}O\text{-}Al^{i}Bu_2]_{feed}$ is the direct consequence of the first-order dependence of the incorporation of $C_{11}{}^{=}O\text{-}Al^{i}Bu_2$ on the $C_{11}{}^{=}O\text{-}Al^{i}Bu_2$ feed concentration, while the difference in the absolute melting temperatures for poly(propylene) and poly(propylene-*co*-undecenol) with the same comonomer ($C_{11}{}^{=}OH$) content is caused by the difference in the regio- and stereo-selectivity of catalysts **1**–**4**. This behavior is clearly governed by the steric hindrance imposed by the Me- and Ph-substituents of the indenyl ligand for catalysts **1** and **3** with melting temperatures of about 20 °C higher compared to the samples produced under identical conditions using catalysts **2** and **4** using the same $C_{11}{}^{=}O\text{-}Al^{i}Bu_2$ feed concentration.

The catalyst structure has a clear effect on the polymer molecular weight and the polydispersity index ($Đ$). Both catalysts bearing substituted indenyl ligands provide higher molecular weights. This is clearly visible when comparing zirconocenes **1** and **2** with higher molecular weights obtained with the substituted indenyl zirconocene **1** (M_n > 80 kg/mol for **1** and M_n < 20 kg/mol for **2**). The trend is less pronounced when comparing hafnocene catalysts **3** and **4** (Figure 4). This is in line with literature reports using these C_2-symmetric silylene-bridged metallocene catalysts in propylene polymerization and ethylene/propylene copolymerization.[36,46] Whereas the molecular weight is mainly governed by the ligand structure, the polydispersity is strongly influenced by the choice of the metal. The zirconocenes clearly show a lower $Đ$ than the isostructural hafnium catalysts (Figure 4B).

Although Figure 3 provides a qualitative picture of the relative ability of **1**–**4** to incorporate $C_{11}{}^{=}O\text{-}Al^{i}Bu_2$, to quantify these results, the reactivity ratios have to be determined. The monomer reactivity ratios in propylene/$C_{11}{}^{=}O\text{-}Al^{i}Bu_2$ copolymerizations were calculated based on the conversions of propylene and $C_{11}{}^{=}OH$ and their respective feed concentrations and incorporation in the copolymer (Chart S1). The results of 4–5 copolymerization experiments with varying $C_{11}{}^{=}O\text{-}Al^{i}Bu_2$ feed concentrations were used to determine the value of the reactivity ratio r_1 applying the following linear methods[47,48]

$$r_1 = \frac{C_3 \text{ conv.}\ (C_{11}\text{ OH conv.} - 1)}{C_{11} \text{ conv.}\ (C_3\text{ OH conv.} - 1)} \quad (1)$$

$$r_1 \frac{[C_{11}{}^{=}O\text{-}Al^{i}Bu_2]_{copol}}{[C_3]_{copol}} = \frac{[C_{11}{}^{=}O\text{-}Al^{i}Bu_2]_{feed}}{[C_3]_{feed}} \quad (2)$$

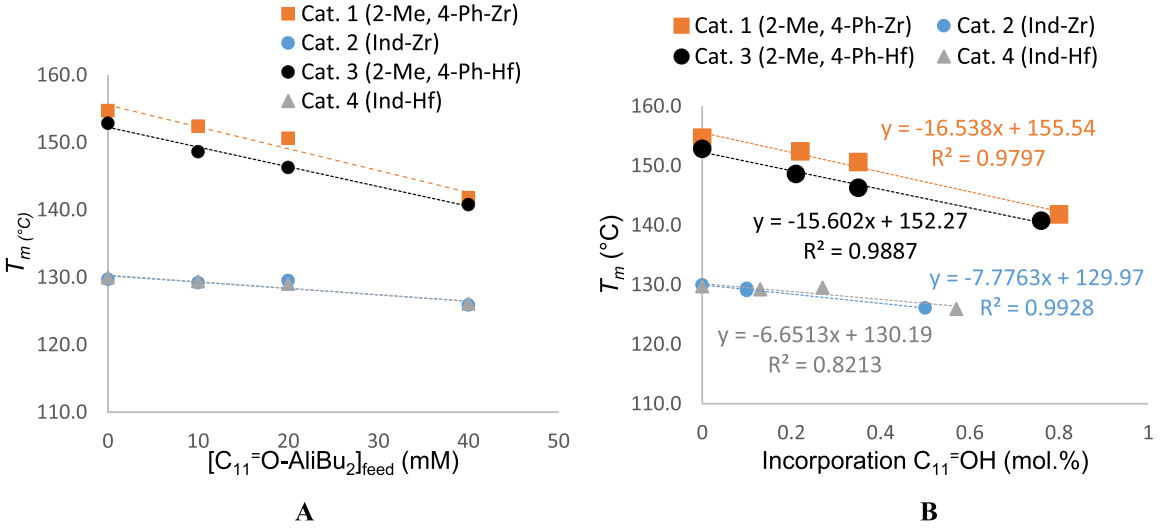

Figure 3. (A) Plot of the melting temperature of poly(propylene-*co*-undecenol) copolymers prepared using catalysts **1**–**4** against the feed concentration of $C_{11}{}^{=}O\text{-}Al^{i}Bu_2$ at 80 °C. (B) Plot of the melting temperature of poly(propylene-*co*-undecenol) copolymers prepared using catalysts **1**–**4** against the incorporation of $C_{11}{}^{=}OH$.

https://doi.org/10.1021/acs.macromol.1c02220
Macromolecules 2022, 55, 776–787

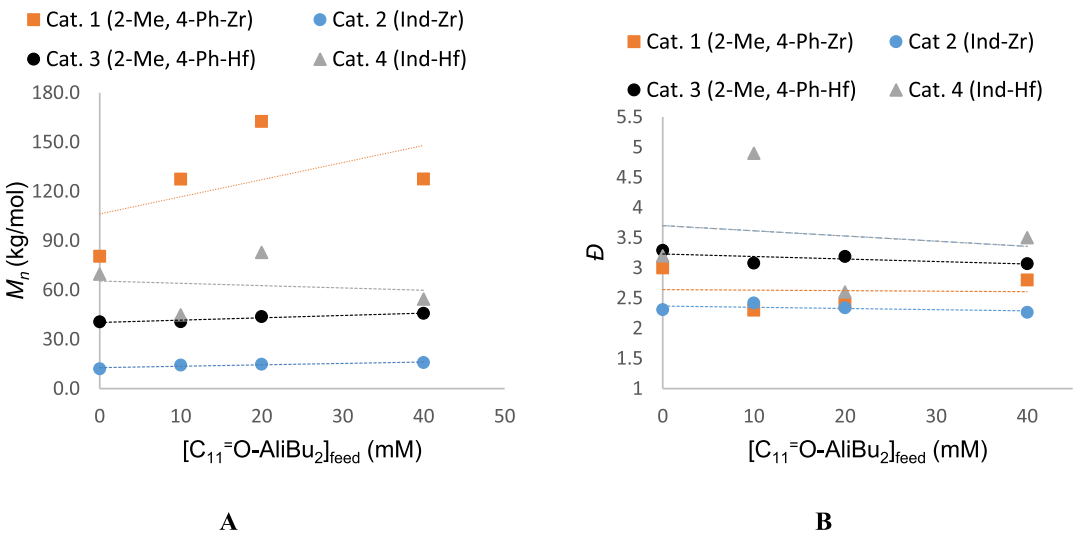

Figure 4. (A) Plot of M_n of poly(propylene-*co*-undecenol) copolymers prepared using catalysts **1**−**4** against the feed concentration of $C_{11}{}^{=}$O-Al^{i}Bu$_2$ at 80 °C. (B) Plot of $Đ$ of poly(propylene-*co*-undecenol) copolymers prepared using catalysts **1**−**4** against the feed concentration of TiBA-$C_{11}{}^{=}$OH at 80 °C.

$$r_1\frac{F^2}{f} = \frac{F(f-1)}{f} \text{ where } F = \frac{[C_3]_{feed}}{[C_{11}{}^{=}\text{O-Al}^i\text{Bu}_2]_{feed}}$$
$$\text{and } f = \frac{[C_3]_{copol}}{[C_{11}{}^{=}\text{O-Al}^i\text{Bu}_2]_{copol}} \quad (3)$$

The reactivity ratios calculated using methods 1−3 are listed in Table 2 and plotted in Figure 5. Interestingly, regardless of the method employed (Table 2), the r_1's show the following order: r_1 (**2**) > r_1 (**4**) > r_1 (**3**) ~ r_1 (**1**). This order clearly indicates the influence of the ligand structure on the relative reactivity of propylene and $C_{11}{}^{=}$O-Al^{i}Bu$_2$, with lower reactivity ratios obtained with the catalysts bearing the substituted indenyl ligands **1** and **3** as compared to **2** and **4**, respectively.

Table 2. Summary of the Reactivity Ratios for Catalysts 1−4 Obtained Using Methods 1−3 in Propylene Copolymerization with $C_{11}{}^{=}$O-Al^{i}Bu$_2$ at 80 °C[a]

	average reactivity ratio r_1		
cat.	method 1[46]	method 2[46]	method 3[47] reactivity ratio r_1
1	2.4 ± 0.4	1.8 ± 0.2	1.5
2	6.5 ± 1.7	3.3 ± 0.4	3.3
3	2.3 ± 0.2	1.9 ± 0.2	1.6
4	4.0 ± 0.7	2.6 ± 0.1	2.8

[a] $C_{11}{}^{=}$O-Al^{i}Bu$_2$ feed concentration used were 10, 20, 30, and 40 mM, respectively.

This is in agreement with the behavior of substituted bis(indenyl) metallocene catalysts in ethylene−α-olefin copolymerizations.[43] Furthermore, the effect of the catalyst's metal center seems to be visible only when comparing the unsubstituted indenyl complexes **2** and **4** with a higher comonomer reactivity displayed by the hafnocene catalyst **4**.

Copolymerization of Propylene with $C_{11}{}^{=}$O-Al^{i}Bu$_2$ Using 1/MMAO at 40−100 °C. Based on the comparison of the catalytic performance of **1**−**4**, zirconocene **1** bearing the substituted 2-Me, 4-Ph indenyl ligand clearly stands out as the best performing catalyst in propylene−$C_{11}{}^{=}$O-Al^{i}Bu$_2$ copolymerization, with a higher catalytic activity, higher molecular weight capability, and enhanced stereo-selectivity and reactivity toward the $C_{11}{}^{=}$O-Al^{i}Bu$_2$ comonomer (a lower r_1 value). Hence, the focus of the rest of this study was directed toward **1**/MMAO as the catalyst system to evaluate its behavior at different temperatures and using different $C_{11}{}^{=}$O-Al^{i}Bu$_2$ feed concentrations. The copolymerization results are presented in Table 3 and Figure 6. In the range of polymerization temperatures from 40 to 90 °C, the catalytic activity gradually increased with increasing temperature. Increasing the temperature further to 100 °C resulted in a drop in the catalytic activity. Keeping in mind that with an increasing temperature from 40 to 100 °C at a constant propylene pressure, the concentration of the dissolved propylene significantly drops (the ratio $[C_3{}^{=}]_{100°C}/[C_3{}^{=}]_{40°C} \approx 0.4$, as determined using the Peng−Robinson equation of state with property parameters from Aspen Plus), the actual rate constant of the polymerization will increase approx. with a factor of 2.5 more than the observed activity obtained under the same propylene pressure. The observed activity at 100 °C was lower than expected, which is either the result of mass transfer limitation at this temperature—meaning that the propylene consumption rate exceeds the propylene dissolution rate—or the result of thermal decomposition of the catalyst. For each polymerization temperature, the catalytic activity is inversely proportional to the $C_{11}{}^{=}$O-Al^{i}Bu$_2$ feed concentration (Figure 6A). This is in agreement with the hypothesis that the oxygen of the $C_{11}{}^{=}$O-Al^{i}Bu$_2$ is still capable to weakly and reversibly coordinate to the highly electrophilic active center. The thus obtained

https://doi.org/10.1021/acs.macromol.1c02220
Macromolecules 2022, 55, 776−787

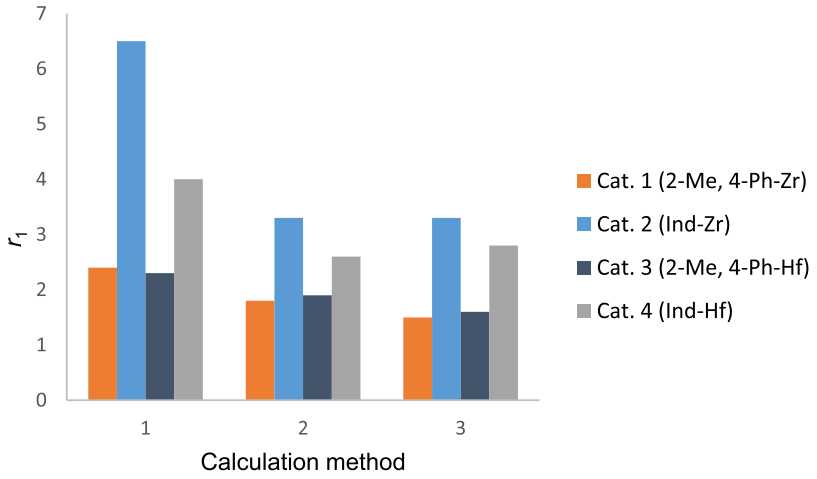

Figure 5. Plot of reactivity ratio r_1 in propylene copolymerization with $C_{11}{=}O\text{-}Al^iBu_2$ obtained at 80 °C with catalysts **1**–**4**/MMAO determined using methods 1–3. See Table 2 for details.

Table 3. Results of Propylene Copolymerization with $C_{11}{=}O\text{-}Al^iBu_2$ Using 1/MMAO as the Catalyst System at Variable Polymerization Temperatures[a]

run #	$C_{11}{=}O\text{-}Al^iBu_2$[b] (mM)	T (°C)	yield (g)	activity (kg mmol cat.$^{-1}$ h^{-1})	M_n[c] (kg mol^{-1})	$Đ$[c]	T_m[d] (°C)	$C_{11}OH$[e] (mol %)
1	0	40	0.9	48	617.3	2.5	160.2	0
2	10	40	2.5	127	872.5	2.0	157.6	0.10
3	20	40	2.1	105	1121.0	1.8	155.5	0.20
4	30	40	2.4	119	1012.0	1.9	154.5	0.32
5	40	40	1.7	85	1008.0	1.9	151.0	0.50
6	0	60	19.9	993	132.1	3.2	158.3	0
7	10	60	6.8	338	454.4	2.1	156.3	0.10
8	20	60	4.3	216	464.4	2.0	152.8	0.38
9	30	60	3.8	191	443.3	2.1	151.5	0.43
10	40	60	2.7	137	441.4	2.2	147.7	0.90
11	0	70	21.8	1090	98.9	3.4	156.8	0
12	10	70	6.0	298	316.6	2.1	154.8	0.20
13	20	70	6.3	315	273.9	2.2	152.2	0.35
14	30	70	3.5	177	275.4	2.2	148.9	0.65
15	40	70	4.1	203	218.2	2.7	147.0	1.00
16	0	80	26.4	1320	80.5	3.0	154.7	0
17	10	80	15.6	782	127.4	2.3	152.4	0.22
18	20	80	5.4	269	162.6	2.4	150.6	0.36
19	30	80	5.8	289	149.9	2.5	146.6	0.70
20	40	80	5.0	252	127.5	2.8	141.8	0.80
21	0	90	26.8	1340	61.7	2.5	154.0	0
22	10	90	19.6	981	63.5	2.7	150.9	0.25
23	20	90	14.9	747	76.5	2.4	148.0	0.40
24	30	90	7.5	374	78.0	2.4	144.8	0.70
25	40	90	3.8	190	77.3	2.5	141.6	0.85
26	0	100	23.4	1170	36.7	2.6	150.0	0
27	10	100	14.7	733	44.7	2.4	148.0	0.25
28	20	100	10.8	535	44.8	2.5	144.8	0.50
29	30	100	5.1	255	46.8	2.5	141.9	0.70
30	40	100	2.6	130	46.0	2.5	138.0	1.05

[a]Conditions: reaction performed in a 600 mL Büchi reactor, 200 mL toluene, propylene pressure = 5 bar, [MMAO]/[cat. **1**] ~ 8300, TiBA (10 wt % solution in toluene) = 2.1 mmol, reaction time = 20 min, cat. **1** = 0.06 μmol. [b]10-Undecen-1-ol ($C_{11}{=}OH$) premixed with TiBA (10 wt % solution in toluene; [TiBA]/[$C_{11}{=}OH$] = 1.1). [c]Determined by HT-SEC in TCB at 160 °C. [d]Determined by DSC. [e]Determined by ^{1}H NMR.

equilibrium of active and dormant catalyst species shifts to the side of dormant species, with an increasing concentration of $C_{11}{=}O\text{-}Al^iBu_2$ in the system.

The synthesized copolymers at different temperatures were characterized using DSC thermal analysis, high-temperature size exclusion chromatography (HT-SEC), and ^{1}H NMR spectroscopy. The DSC data are presented in Table 3 and plotted in Figure 6B, and the individual DSC thermographs are presented in Figures S6–S11. The melting temperature development of poly(propylene-*co*-undecenol) against the feed concentration of $C_{11}{=}O\text{-}Al^iBu_2$ at polymerization temperatures ranging from 40 to 100 °C shows a linear inversely

https://doi.org/10.1021/acs.macromol.1c02220
Macromolecules 2022, 55, 776–787

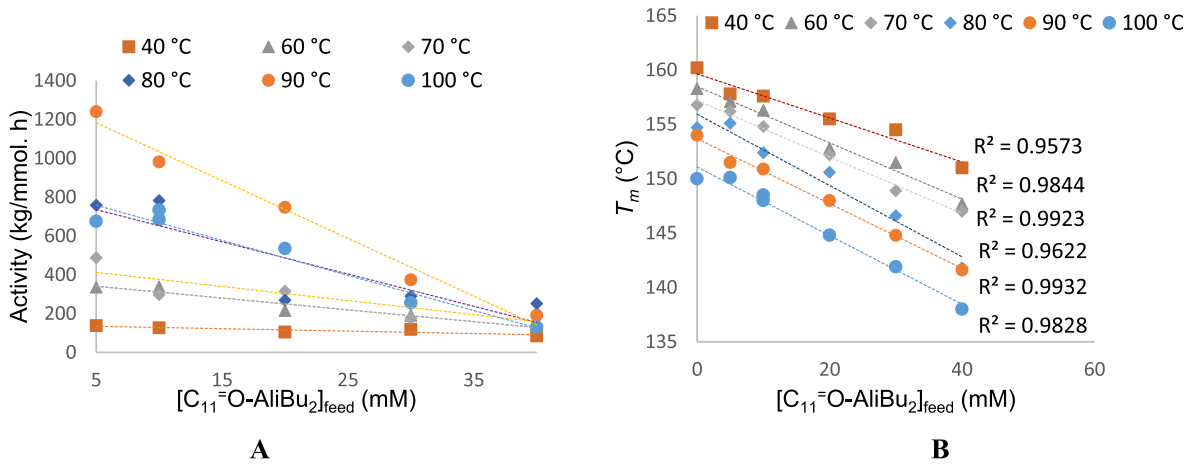

Figure 6. Plots of (A) catalytic activities and (B) melting temperatures of poly(propylene-*co*-undecenol) of **1**/MMAO against the feed concentration of $C_{11}^{=}$O-Al^{i}Bu$_2$ (mM) at variable polymerization temperatures.

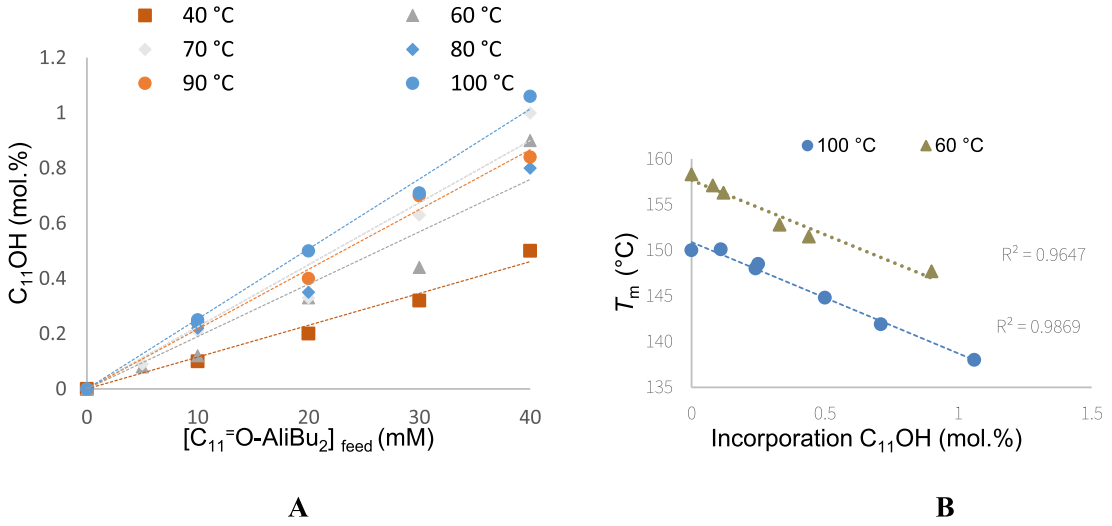

Figure 7. (A) Plot of $C_{11}^{=}$OH incorporation (mol %) against the feed concentration of $C_{11}^{=}$O-Al^{i}Bu$_2$ (0−40 mM). (B) Plot of the melting temperatures of poly(propylene-*co*-undecenol) against the $C_{11}^{=}$OH content (mol %) in copolymers produced at 60 and 100 °C.

proportional relationship, which is in line with first-order kinetics and provides clear evidence of the increased incorporation of the $C_{11}^{=}$OH comonomer with an increasing $C_{11}^{=}$O-Al^{i}Bu$_2$ feed concentration. This was confirmed by ^{1}H NMR analysis showing a linear relationship between $C_{11}^{=}$OH incorporation and its initial feed concentration (Table 3 and Figure 7A). The fact that the $C_{11}^{=}$O-Al^{i}Bu$_2$ incorporation increases with increasing polymerization temperature (Figure 7A) can be explained by the decreasing propylene concentration (higher $C_{11}^{=}$O-Al^{i}Bu$_2$/propylene ratio) upon increasing the polymerization temperature while keeping the propylene pressure constant.

Furthermore, the melting temperatures of poly(propylene-*co*-undecenol) copolymers listed in Table 3 were plotted against the comonomer content determined by ^{1}H NMR (Figure 7B). The inverse linear correlations (T_m vs C_{11}OH content) of the samples produced at 60 and 100 °C show a similar slope (∼−12), which indicates a linear dependency of the melting temperatures of poly(propylene-*co*-undecenol) on the comonomer content irrespective of the polymerization temperature. The difference in the absolute T_m values for homopolymers or copolymers containing the same amount of $C_{11}^{=}$OH (mol %) produced at 60 and 100 °C of approx. 8 °C results from the difference in the stereo/region errors occurring at increasing extents when increasing the polymerization temperature.

The HT-SEC analysis of the copolymers produced at different temperatures and $C_{11}^{=}$O-Al^{i}Bu$_2$ feed concentrations showed that the amount of $C_{11}^{=}$O-Al^{i}Bu$_2$ in the feed has no effect on the copolymer's molecular weight, whereas the increase in polymerization temperature resulted in a significant drop of poly(propylene-*co*-undecenol) molecular weight (Figure 8). The latter can be explained by the decreasing propylene concentration (at a fixed propylene pressure of 5 bar) and the decreasing $\Delta E_{activation}$ between the chain transfer and the chain growth with increasing temperature.

To allow a meaningful comparison of the polymerization data obtained using **1**/MMAO at variable temperatures, the reactivity ratio of propylene and $C_{11}^{=}$O-Al^{i}Bu$_2$ was calculated using methods 1−3 at corrected propylene concentrations determined using the Peng−Robinson equation of state with property parameters from Aspen Plus versus the polymerization temperatures (Table 4 and Figure 9). From Figure 9, it is evident that the polymerization temperature has a significant effect on the reactivity ratio of propylene/$C_{11}^{=}$O-Al^{i}Bu$_2$ with a steady drop of r_1 as a function of polymerization temperature,

https://doi.org/10.1021/acs.macromol.1c02220
Macromolecules 2022, 55, 776−787

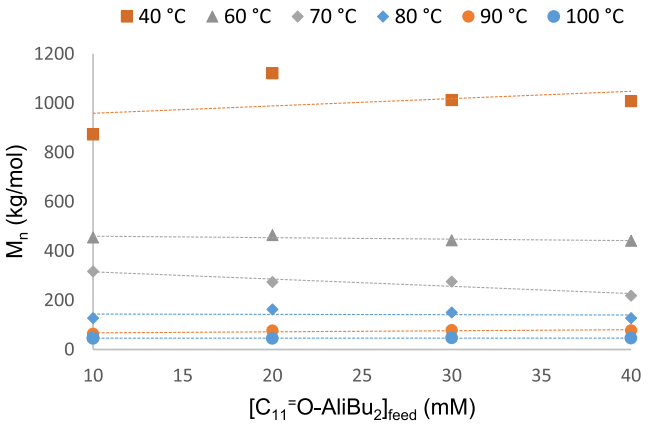

Figure 8. Plots of M_n (kg mol^{-1}) of poly(propylene-*co*-undecenol) copolymers produced using a **1**/MMAO vs C_{11}=O-Al^{i}Bu$_2$ feed concentration (mM) at variable polymerization temperatures.

Table 4. Summary of Reactivity Ratios for Catalyst 1/MMAO Obtained Using Methods 1−3 in Propylene Copolymerization with C_{11}=O-Al^{i}Bu$_2$ Using the Corrected Propylene Concentrations Derived from Aspen Plus at Six Polymerization Temperatures from 40 to 100 °C[a]

	average reactivity ratio r_1		
temperature	method 1	method 2	method 3 reactivity ratio r_1
40	3.4 ± 0.4	3.2 ± 0.3	2.8
60	2.7 ± 1.3	2.3 ± 0.9	2.7
70	1.9 ± 0.4	1.7 ± 0.3	1.7
80	2.2 ± 0.5	1.7 ± 0.2	1.6
90	2.1 ± 1.0	1.6 ± 0.2	1.5
100	1.8 ± 0.3	1.5 ± 0.1	1.4

[a] $[C_{11}$=O-Al^{i}Bu$_2]_{feed}$ = 10, 20, 30 and 40 mM.

indicating that catalyst **1** has an increasing reactivity toward the C_{11}=O-Al^{i}Bu$_2$ comonomer upon increasing polymerization temperature. This can be explained by the decreasing $\Delta E_{activation}$ for the insertion reaction of C_{11}=O-Al^{i}Bu$_2$ versus propylene with increasing polymerization temperature, which is in line with literature reports describing the same behavior of metallocene catalysts in ethylene/α-olefins[43] and ethylene/alkenol copolymerization.[49]

To evaluate the potential of **1** in producing hydroxyl-functionalized polypropylenes under industrially relevant process conditions, the performance of **1** in propylene copolymerization with hydroxyl-functionalized α-olefins was carried out under solution process conditions (130−150 °C) and under slurry- and gas-phase process conditions (85 °C) using a silica-supported version of **1**. The silica-supported catalyst **1** was first used in the gas-phase propylene copolymerization with 10-undecen-1-ol (C_{11}=OH) premixed with an equimolar amount of TiBA and the corresponding results are listed in Table S4. Acceptable tolerance to TiBA-passivated 10-undecen-1-ol can be observed, and high-molecular-weight products were obtained (M_n > 50 kg/mol). However, DSC and NMR analyses did not show any evidence of C_{11}=OH incorporation with melting temperatures comparable to the reference polypropylene homopolymer. This was first accredited to the reduced volatility of TiBA-passivated C_{11}=OH under the gas-phase reaction conditions; however, the copolymerization trials conducted using the same silica-supported catalyst under slurry-phase conditions in propylene/C_{11}=O-Al^{i}Bu$_2$ copolymerization resulted in the same outcome. The lack of affinity or incorporation ability of this silica-supported catalyst toward TiBA−C_{11}=OH, combined with the absence of catalyst poisoning, suggests that C_{11}=O-Al^{i}Bu$_2$ is too sterically hindered to migrate to the active sites of the heterogeneous catalyst and/or is effectively adsorbed onto the catalyst support. Unfortunately, attempts using non-porous solid MAO (Tosoh Finechem Corporation) as the support did not lead to better results, and replacing TiBA with trimethyl aluminum to afford the less sterically hindered C_{11}=O-AlMe$_2$ resulted in catalyst deactivation. To elucidate the exact cause of the lack of incorporation of C_{11}=O-Al^{i}Bu$_2$ once silica supported **1** is applied, an in-depth study requiring dedicated methods and expertise (surface science, computational methods, etc.) has to be conducted, which falls outside the scope of this paper.

Next, the performance of the unsupported catalyst **1**/MAO was evaluated at 130−150 °C in propylene copolymerization with C_{11}=O-Al^{i}Bu$_2$. The propylene polymerization conducted with C_3= pressures of 5 and 15 bar (to compensate for the

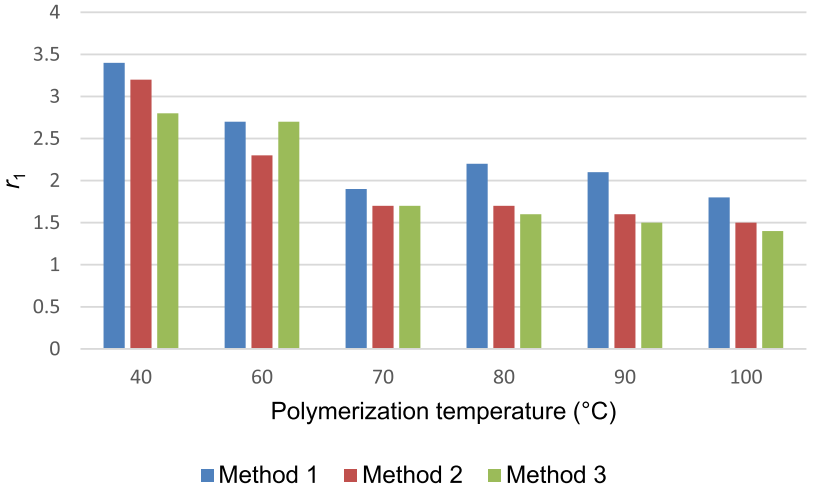

Figure 9. Plot of reactivity ratio r_1 in propylene/C_{11}=O-Al^{i}Bu$_2$ copolymerization catalyzed by **1**/MMAO obtained with corrected propylene concentrations at six different temperatures ranging from 40 to 100 °C using methods 1−3.

https://doi.org/10.1021/acs.macromol.1c02220
Macromolecules 2022, 55, 776−787

lower solubility of propylene at higher temperatures) results indicate clearly the limited molecular weight capability and stereo-selectivity of catalyst **1** at elevated temperatures with $M_n \leq 5$ kg/mol (5 bar $C_3^=$) and ≤20 kg/mol (15 bar $C_3^=$) and T_m's far below those obtained at 80 °C (Table S5). While being a suitable catalyst for lab screening, catalyst **1** shows severe limitations under industrially relevant process conditions.

CONCLUSIONS

This study demonstrates the effect of the catalyst structure and polymerization temperature on the catalytic performance of C_2-symmetric silylene-bridged zirconocenes and hafnocenes during the copolymerization of propylene and TiBA-passivated 10-undecen-1-ol. The kinetic study revealed a noticeable influence of the catalyst's metal center with higher catalytic activities obtained using the zirconocenes (**1** and **2**) than analogous hafnocenes (**2** and **4**) during propylene/$C_{11}^=$O-Al^{i}Bu$_2$ copolymerization. It was found that the substituted indenyl zirconocene (**1**) and hafnocene (**3**) catalysts afford higher comonomer reactivity and stereo-selectivity compared to their non-substituted congeners (**2** and **4**). As expected, a linear relationship between the polymerization temperature versus copolymer molecular weight and melting temperature exists. More importantly, the highly active and iso-selective zirconocene catalyst **1** exhibited an outstanding ability to incorporate the hydroxyl-functionalized α-olefin with an increasing comonomer reactivity upon increasing polymerization temperature, making **1** a catalyst of choice for producing functionalized polyolefins.

On the other hand, the polypropylene functionalization study conducted using this outstanding catalyst under industrially relevant gas-phase and solution process conditions revealed its limited potential to be used as a catalyst for producing hydroxyl-functionalized polypropylene applying the existing polyolefin commercial process technologies with the lack of functionality under gas-phase conditions and limited molecular weight capability and stereo-selectivity at elevated temperatures required in a solution process.

ASSOCIATED CONTENT

Supporting Information

The Supporting Information is available free of charge at https://pubs.acs.org/doi/10.1021/acs.macromol.1c02220.

Optimization of propylene polymerization conditions using pre-catalyst *rac*-Me$_2$Si(2-Me-4-Ph-Ind)$_2$ZrCl$_2$ (**1**), additional polymerization experiments, plots of polymerization activities, MW, T_m, activation energy, DSC thermographs, NMR spectra, and reactivity ratios (PDF)

AUTHOR INFORMATION

Corresponding Authors

Miloud Bouyahyi − *SABIC Technology & Innovation, 6167 RD Geleen, The Netherlands;* orcid.org/0000-0001-7466-6671; Email: Miloud.Bouyahyi@SABIC.com

Rob Duchateau − *SABIC Technology & Innovation, 6167 RD Geleen, The Netherlands; Engineering and Technology Institute Groningen, University of Groningen, 9747 AG Groningen, The Netherlands;* orcid.org/0000-0002-2641-4354; Email: Rob.Duchateau@SABIC.com

Muhammad Naseem Akhtar − *Center for Refining and Advanced Chemicals, Research Institute, King Fahd University of Petroleum & Minerals, 31261 Dhahran, Saudi Arabia*; Email: mnakhtar@kfupm.edu.sa

Authors

Lidia Jasinska-Walc − *SABIC Technology & Innovation, STC Geleen, 6167 RD Geleen, The Netherlands; Department of Chemistry and Technology of Functional Materials, Chemical Faculty, Gdansk University of Technology, 80-233 Gdansk, Poland;* orcid.org/0000-0001-6793-6936

E. A. Jaseer − *Center for Refining and Advanced Chemicals, Research Institute, King Fahd University of Petroleum & Minerals, 31261 Dhahran, Saudi Arabia;* orcid.org/0000-0002-5385-8778

Rajesh Theravalappil − *Center for Refining and Advanced Chemicals, Research Institute, King Fahd University of Petroleum & Minerals, 31261 Dhahran, Saudi Arabia*

Nestor Garcia − *Center for Refining and Advanced Chemicals, Research Institute, King Fahd University of Petroleum & Minerals, 31261 Dhahran, Saudi Arabia*

Complete contact information is available at: https://pubs.acs.org/10.1021/acs.macromol.1c02220

Notes

The authors declare no competing financial interest.

ACKNOWLEDGMENTS

The authors would like to acknowledge the support provided by SABIC for funding the project # CRP02278 at the Center for Refining and Advanced Chemicals (CRAC)/RI-KFUPM. The support of King Fahd University of Petroleum & Minerals (KFUPM), Dhahran, Saudi Arabia, is also highly appreciated.

REFERENCES

(1) IHS Market. *Polypropylene Edition 2017*, 2018.

(2) Hustad, P. D. Frontiers in Olefin Polymerization: Reinventing the World's Most Common Synthetic Polymers. *Science* **2009**, *325*, 704−707.

(3) Röttger, M.; Domenech, T.; van der Weegen, R.; Breuillac, A.; Nicolay, R.; Leibler, L. High Performance Vitrimers from Commodity Thermoplastics through Dioxaborolane Metathesis. *Science* **2017**, *356*, 62−65.

(4) Amin, S. B.; Marks, T. J. Versatile Pathways for In Situ Polyolefin Functionalization with Heteroatoms: Catalytic Chain Transfer. *Angew. Chem., Int. Ed.* **2008**, *47*, 2006−2025.

(5) Chung, T. C. *Functionalisation of Polyolefins*; Academic Press: London, 2002.

(6) Franssen, N. M. G.; Reek, J. N. H.; de Bruin, B. Synthesis of Functional Polyolefins: State of the Art and Remaining Challenges. *Chem. Soc. Rev.* **2013**, *42*, 5809−5832.

(7) Peacock, A. J. *Handbook of Polyethylene, Structure, Properties and Applications*; Marcel Dekker, Inc., 2000.

(8) Boaen, N. K.; Hillmyer, M. A. Post-Polymerization Functionalization of Polyolefins. *Chem. Soc. Rev.* **2005**, *34*, 267−275.

(9) Moad, G. The Synthesis of Polyolefin Graft Copolymers by Reactive Extrusion. *Prog. Polym. Sci.* **1999**, *24*, 81−142.

(10) Boffa, L. S.; Novak, B. M. Copolymerization of Polar Monomers with Olefins using Transition-Metal Complexes. *Chem. Rev.* **2000**, *100*, 1479−1494.

(11) Dong, J.-Y.; Hu, Y. Design and Synthesis of Structurally Well-Defined Functional Polyolefins via Transition Metal-Mediated Olefin Polymerization Chemistry. *Coord. Chem. Rev.* **2006**, *250*, 47−65.

(12) Fan, G.; Dong, J.-Y. An Examination of Aluminum Chain Transfer Reaction in rac-Me$_2$Si[2-Me-4-Naph-Ind]$_2$ZrCl$_2$/MAO-catalyzed Propylene Polymerization and Synthesis of Aluminum-terminated Isotactic Polypropylene with Controlled Molecular Weight. *J. Mol. Catal. A: Chem.* **2005**, *236*, 246−252.

(13) Ring, J. O.; Thomann, R.; Mülhaupt, R.; Raquez, J.-M.; Degée, P.; Dubois, P. Controlled Synthesis and Characterization of Poly[ethylene-block-(L,L-lactide)]s by Combining Catalytic Ethylene Oligomerization with "Coordination-Insertion" Ring-Opening Polymerization. *Macromol. Chem. Phys.* **2007**, *208*, 896−902.
(14) For example, see: Kay, C. J.; Goring, P. D.; Burnett, C. A.; Hornby, B.; Lewtas, K.; Morris, S.; Morton, C.; McNally, T.; Theaker, G. W.; Waterson, C.; Wright, P. M.; Scott, P. Polyolefin−Polar Block Copolymers from Versatile new Macromonomers. *J. Am. Chem. Soc.* **2018**, *140*, 13921−13934.
(15) For example, see: Chung, T. C.; Lu, H. L. Functionalization and Block Reactions of Polyolefins using Metallocene Catalysts and Borane Reagents. *J. Mol. Catal. A: Chem.* **1997**, *115*, 115−127.
(16) For example, see: Shiono, T.; Sugimoto, M.; Hasan, T.; Cai, Z. Facile Synthesis of Hydroxy-Functionalized Cycloolefin Copolymer Using ω-Alkenylaluminium as a Comonomer. *Macromol. Chem. Phys.* **2013**, *214*, 2239−2244.
(17) For example, see: Goretzki, R.; Fink, G. Homogeneous and Heterogeneous Metallocene/MAO-catalyzed Polymerization of Trialkylsilyl-protected Alcohols. *Macromol. Rapid Commun.* **1999**, *19*, 511−515.
(18) Hakala, K.; Helaja, T.; Lofgren, B. Metallocene/methyl aluminoxane-catalyzed Copolymerizations of Oxygen-functionalized Long-chain Olefins with Ethylene. *J. Polym. Sci., Part A: Polym. Chem.* **2000**, *38*, 1966−1971.
(19) For example, see: Goretzki, R.; Fink, G. Homogeneous and Heterogeneous Metallocene/MAO-Catalyzed Polymerization of Functionalized Olefins. *Macromol. Chem. Phys.* **1999**, *200*, 881−886.
(20) Aaltonen, P.; Loefgren, B. Synthesis of Functional Polyethylenes with Soluble Metallocene/Methylaluminoxane Catalyst. *Macromolecules* **1995**, *28*, 5353−5357.
(21) Bouyahyi, M.; Turki, Y.; Tanwar, A.; Jasinska-Walc, L.; Duchateau, R. Randomly Functionalized Polyethylenes: In Quest of Avoiding Catalyst Deactivation. *ACS Catal.* **2019**, *9*, 7779−7790.
(22) Wilén, C.-E.; Luttikhedde, H.; Hjertberg, T.; Näsman, J. H. Copolymerization of Ethylene and 6-tert-Butyl-2-(1,1-dimethylhept-6-enyl)-4-methylphenol over Three Different Metallocene-Alumoxane Catalyst Systems. *Macromolecules* **1996**, *29*, 8569−8575.
(23) Dong, J. Y.; Chung, T. C. Synthesis of Polyethylene Containing a Terminal p-Methylstyrene Group: Metallocene-Mediated Ethylene Polymerization with a Consecutive Chain Transfer Reaction to p-Methylstyrene and Hydrogen. *Macromolecules* **2002**, *35*, 1622−1631.
(24) Yang, X.-H.; Liu, C.-R.; Wang, C.; Sun, X.-L.; Guo, Y.-H.; Wang, X.-K.; Wang, Z.; Xie, Z.; Tang, Y. [ONSR]$TiCl_3$-Catalyzed Copolymerization of Ethylene with Functionalized Olefins. *Angew. Chem., Int. Ed.* **2009**, *48*, 8099−8102.
(25) Hakala, K.; Löfgren, B.; Helaja, T. Copolymerizations of Oxygen-Functionalized Olefins with Propylene using Metallocene/Methylaluminoxane Catalyst. *Eur. Polym. J.* **1998**, *34*, 1093−1097.
(26) Marques, M. M.; Correia, S. G.; Ascenso, J. R.; Ribeiro, A. F. G.; Gomes, P. T.; Dias, A. R.; Foster, P.; Rausch, M. D.; Chien, J. C. W. Polymerization with TMA-Protected Polar Vinyl Comonomers. I. Catalyzed by Group 4 Metal Complexes with η5-type Ligands. *J. Polym. Sci. Part A: Polym. Chem.* **1999**, *37*, 2457−2469.
(27) Song, S.; Zhang, Z.; Liu, X.; Fu, Z.; Xu, J.; Fan, Z. Synthesis and Characterization of Functional Polyethylene with Regularly Distributed Thioester Pendants via Ring-Opening Metathesis Polymerization. *J. Polym. Sci., Part A: Polym. Chem.* **2017**, *55*, 4027−4036.
(28) For example, see: Morishita, H.; Sudo, A.; Endo, T. Synthesis and Palladium-Catalyzed Addition Polymerization of Norbornene Carrying Epoxy Moiety. *J. Polym. Sci., Part A: Polym. Chem.* **2009**, *47*, 3982−3989.
(29) Kwasny, M. T.; Watkins, C. M.; Posey, N. D.; Matta, M. E.; Tew, G. N. Functional Polyethylenes with Precisely Placed Thioethers and Sulfoniums through Thiol-Ene Polymerization Comonomers. *Macromolecules* **2018**, *51*, 4280−4289.
(30) Shang, R.; Gao, H.; Luo, F.; Li, Y.; Wang, B.; Ma, Z.; Pan, L.; Li, Y. Functional Isotactic Polypropylenes via Efficient Direct Copolymerizations of Propylene with Various Amino-Functionalized α-Olefins. *Macromolecules* **2019**, *52*, 9280−9290.
(31) Huang, M.; Chen, J.; Wang, B.; Huang, W.; Chen, H.; Gao, Y.; Marks, T. J. Polar Isotactic and Syndiotactic Polypropylenes via Organozirconium-Catalyzed Masking-Reagent-Free Propylene and Amino-Olefin Copolymerization. *Angew. Chem., Int. Ed.* **2020**, *59*, 20522−20528.
(32) Chen, J.; Gao, Y.; Wang, B.; Lohr, T. L.; Marks, T. J. Scandium-Catalyzed Self-Assisted Polar Co-monomer Enchainment in Ethylene Polymerization. *Angew. Chem., Int. Ed.* **2017**, *56*, 15964−15968.
(33) Wang, C.; Luo, G.; Nishiura, M.; Song, G.; Yamamoto, A.; Luo, Y.; Hou, Z. Heteroatom-assisted Olefin Polymerization by Rare-Earth Metal Catalysts. *Sci. Adv.* **2017**, *3*, No. e1701011.
(34) For example, see: Zhang, X.; Chen, S.; Li, H.; Zhang, Z.; Lu, Y.; Wu, C.; Hu, Y. Copolymerizations of Ethylene and Polar Comonomers with Bis(phenoxyketimine) Group IV Complexes: Effects of the Central Metal Properties. *J. Polym. Sci., Part A: Polym. Chem.* **2006**, *45*, 59−68.
(35) Spaleck, W.; Kueber, F.; Winter, A.; Rohrmann, J.; Bachmann, B.; Antberg, M.; Dolle, V.; Paulus, E. F. The Influence of Aromatic Substituents on the Polymerization Behavior of Bridged Zirconocene Catalysts. *Organometallics* **1994**, *13*, 954−963.
(36) Ehm, C.; Vittoria, A.; Goryunov, G. P.; Izmer, V. V.; Kononovich, D. S.; Kulyabin, P. S.; Di Girolamo, R.; Budzelaar, P. H. M.; Voskoboynikov, A. Z.; Busico, V.; Uborsky, D. V.; Cipullo, R. A Systematic Study of the Temperature-Induced Performance Decline of ansa-Metallocenes for iPP. *Macromolecules* **2020**, *53*, 9325−9336.
(37) Desert, X.; Proutiere, F.; Welle, A.; Den Dauw, K.; Vantomme, A.; Miserque, O.; Brusson, J.-M.; Carpentier, J.-F.; Kirillov, E. Zirconocene-Catalyzed Polymerization of a-Olefins: When Intrinsic Higher Activity Is Flawed by Rapid Deactivation. *Organometallics* **2019**, *38*, 2664−2673.
(38) Ehm, C.; Vittoria, A.; Goryunov, G. P.; Izmer, V. V.; Kononovich, D. S.; Samsonov, O. V.; Budzelaar, P. H. M.; Voskoboynikov, A. Z.; Uborsky, D. V.; Cipullo, R. On the Limits of Tuning Comonomer Affinity of 'Spaleck-type' Ansa-Zirconocenes in Ethene/1-Hexene Copolymerization: a High-Throughput Experimentation/QSAR Approach. *Dalton Trans.* **2020**, *49*, 10162−10172.
(39) Zhang, M.; Colby, R. H.; Milner, S. T.; Chung, T. C. M.; Huang, T.; deGroot, W. Synthesis and Characterization of Maleic Anhydride Grafted Polypropylene with a Well-Defined Molecular Structure. *Macromolecules* **2013**, *46*, 4313−4323.
(40) Ginzburg, A.; Ramakrishnan, V.; Rongo, L.; Rozanski, A.; Bouyahyi, M.; Jasinska-Walc, L.; Duchateau, R. The Influence of Polypropylene-Block/Graft-Polycaprolactone Copolymers on Melt Rheology, Morphology, and Dielectric Properties of Polypropylene/Polycarbonate Blends. *Rheo. Act.* **2020**, *59*, 601−619.
(41) Nyangoye, B. O.; Li, T.; Chen, L.; Cai, Z. Reactivity Comparison of ω-Alkenols and Higher 1-Alkenes in Copolymerization with Propylene using an Isospecific Zirconocene-MMAO Catalyst. *Polymers* **2015**, *7*, 2009−2016.
(42) Hendriksen, C.; Friederichs, F.; Sainani, J. B.; Chatteree, A.; Izmer, V.; Kononovich, D.; Voskoboynikov, A.; Busico, V.; Cipullo, R.; Vittoria, A. WO 2020043815 A1, SABIC Global Technologies B.V, 2020.
(43) Kaminsky, W., Eds.; Polyolefins: 50 Years after Ziegler and Natta II-Polyolefins by Metallocenes and other Single-Site Catalysts. *Adv. Pol. Sci.* Vol. *258*, Springer, Berlin, Heidelberg.
(44) Chien, J. C. W.; He, D.; He, D. Olefin Copolymerization with Metallocene Catalysts. I. Comparison of Catalysts. *J. Polym. Sci., Part A: Polym. Chem.* **1991**, *29*, 1585−1593.
(45) Heiland, K.; Kaminsky, W. Comparison of Zirconocene and Hafnocene Catalysts for the Polymerization of Ethylene and 1-Butene. *Makromol. Chem.* **1992**, *193*, 601−610.
(46) Karssenberg, F. G.; Wang, B.; Friederichs, N.; Mathot, V. B. F. Terminal and Penultimate Reactivity Ratios in Single-Site Ethene/Propene Copolymerizations: Comparison of Kakugo and Direct Peak Methods. *Macromol. Chem. Phys.* **2005**, *206*, 1675−1683.

https://doi.org/10.1021/acs.macromol.1c02220
Macromolecules 2022, 55, 776−787

(47) For methods 1−2, see for example: Kissin, Y.; Brandolini, A.; Garlick, J. L. Kinetics of Ethylene Polymerization Reactions with Chromium Oxide Catalysts. *J. Polym. Sci., Part A: Polym. Chem.* **2008**, *46*, 5315−5329.
(48) For method 3, see: Fineman, M.; Ross, S. D. Linear Method for Determining Monomer Reactivity Ratios in Copolymerization. *J. Polym. Sci.* **1950**, *5*, 259−262.
(49) Aaltonen, P.; Fink, G.; Löfgren, B.; Seppälä, J. Synthesis of Hydroxyl Group Containing Polyolefins with Metallocene/Methylaluminoxane Catalysts. *Macromolecules* **1996**, *29*, 5255−5260.

https://doi.org/10.1021/acs.macromol.1c02220
Macromolecules 2022, 55, 776−787